Enhancing Mass Transport in Jet Electrode to Study Highly Active Enzymes

Mariam Fadel*[a,b], Jean-Vincent Daurelle[a], Vincent Fourmond[b], Jerome Vicente[a]

[a]Aix Marseille Université (AMU) Laboratoire IUSTI (UMR AMU-CNRS 7343) Polytech Marseille, Dpt Mécanique Energétique (ME) Technopôle de Chateau Gombert 5 rue Enrico Fermi 13453 Marseille cedex 13, France.
[b]Laboratoire de Bioénergétique et Ingénierie des Protéines, Institut de Microbiologie de la Méditerranée,UMR 7281 Aix-Marseille Université/CNRS, 31 Chemin J. Aiguier, 13402 Marseille Cedex 20, France.
Mariam Fadel*: mariam.fadel@etu.univ-amu.fr

Résumé :

CO- déshydrogénase est une enzyme qui présente un très fort potentiel pour la production de combustible par conversion catalytique du CO2 [1]. *L'électrode à disque tournant (RDE) traditionnellement utilisée pour l'analyse de la cinétique des réactions par électrochimie directe est presque inopérante sur cette enzyme particulièrement active* [2]. *En effet, la RDE ne génère pas un transport suffisant d'espèces réactives sur la surface de l'électrode. Pour surmonter cette limitation, à l'aide de simulations numériques, nous avons mené une étude comparative des principales technologies de cellules électrochimiques. Nous proposons une géométrie d'électrode à jet particulièrement adaptée aux contraintes posées par ces enzymes.*

Abstract :

CO-dehydrogenase is a very promising enzyme for production of fuel from renewable resources by catalytic conversion of carbon dioxide [1]. *The rotating disk electrode (RDE) classically used for the analysis of the kinetics reactions by direct electrochemistry, is almost inoperative on this particularly active enzyme* [2]. *Indeed, the RDE does not generate sufficient transport of reactive species on the surface of the electrode. To overcome this limitation, using numerical simulations, we carried out a comparative study of the main electrochemical cell technologies. We propose a jet electrode geometry particularly adapted to the constrains posed by these enzymes.*

Keywords: Mass Transport; Numerical Simulation; Diffusion; Electrode

1. Introduction

For good investigation of chemical processes performed at the electrode surface, the system should not be limited by transport. The main use of hydrodynamics electrodes is to enhance the mass transport of the reactive species toward the electrode. The rotating disk electrode (RDE) is the most popular hydrodynamic electrode, particularly, in studying the kinetics of the electrochemical processes [3,4].

However, this classical electrochemical cell (RDE), in certain cases, like working with highly active enzymes such as CO dehydrogenase, the transport toward the reactive part disk of electrode, is insufficient. This induces difficulties to study the kinetic mechanism of the enzymatic catalytic reaction. Even though other types of electrodes are presented, the fluid motion depends on an imposed flow either perpendicular to the electrode surface (active site) called as jet flow or radially called as channel flow. The greatly applied forms of these geometries go their ways in the analytical fields and electroanaylsis sensors [5,6]. Such types of these hydrodynamics electrodes are rarely applied for the kinetic mechanistic studies, and none for the study of the kinetic activity of enzymes used in chemical catalytic processes.

Herein, the focus is what happening in the close vicinity of the electrode, since the concentration gradients due to the electrochemical reactions are mostly located in this region [7]. The phenomenon that dominates this region is the diffusion process that occurs in the diffusion boundary layer. This layer should be small enough for the system to be under catalytic kinetic control. Thus, the recorded measurements will interpret the kinetic mechanisms of such chemical reactions performed at the reactive electrode surface.

To implement our numerical tools, we simulate the convection-diffusion process and compare our model with different results in the literature as well as the analytical solutions. We show that our model describes well the phenomena measured by our experimental cell.

In this article, at first, we illustrate the limits of use of RDE cell. Then, to overcome this issue, a bibliographic study of the main electrochemical cell technologies allows us to identify the geometries that are most adapted to our problem; intensify the flow of species while homogenizing its distribution at the surface of the electrode and limiting the washing of the enzyme.

2. Main Convective-Diffusion Equations Applied to RDE:

The equations governing the flow in the vicinity of a rotating disc electrode immersed in a bath were described by Von Karman and then by Cochran [9]. They establish the velocity profiles in the vicinity of the electrode, assuming that the disk is infinite and that the velocity is constant away from the electrode [3]. Based on these assumptions, Levich proposes a solution to the diffusion equation. In this case, the concentration is assumed to be constant outside the boundary layer, which is verified experimentally by convection movements in the bath. According to the first Fick scattering law, the flux, j, and the concentration of the species can be expressed at any point (z) as [3,4] :

$$1) \quad j = D\frac{C_{bulk}-C_0}{\delta}$$

With the hypotheses mentioned, the convection-diffusion equation applied to the RDE system reduces to:

$$2) \quad \frac{\partial C_j}{\partial t} = D_j\frac{\partial^2 C_j}{\partial z^2} - v_z\frac{\partial C_j}{\partial z}$$

In Fick's 2nd law of convective and diffusion equation, the gradient concentration is dependent on the axial velocity v_z, since $\frac{\partial C_0}{\partial r} = \frac{\partial C_0}{\partial \theta} = 0$ for all z. The axial velocity, v_z, is the velocity component normal to the electrode, is independent of the radial and swirl coordinates and only dependent on z. [4].

At z=0; C_0=0 and far away from the electrode C=C_{bulk}, the equation of the concentration will be as:

$$3) \quad \frac{\partial C_0}{dz}_{z=0} = \frac{[C]_{atthebulk}-[C]_{(z=0)}}{\delta}$$

Levich establishes the diffusion boundary layer thickness, δ, in function of the rotating speed, the diffusion coefficient, D, and the viscosity of the fluid, ν, and are written as:

$$4) \quad \delta_{RDE} = 1.61(\omega)^{\frac{-1}{2}}(\nu)^{\frac{1}{6}}D^{1/3}$$

3. Numerical Model of RDE

We simulate the RDE cell used in our experimental work in order to validate our numerical model but also to show that this electrode cannot meet our needs on the study of dehydrogenases. The electrode consists of a disk that includes the reactive area made of conductive material (graphite, carbon etc.) as shown in Figure 1(a). We will consider the radius of this reactive part as the radius of electrode and symbolized it by R, (R=1.5 mm). This electrode is dipped inside the cell bath (Figure 1(a)). The simulations are done using software Starccm+ from CD-ADAPCO based on the finite volume method. Here, to compute precisely the diffusion and the flow near the electrode bottom surface, the mesh size must be smaller than the boundary layer thickness. We create a mesh size of 5.10^{-6} m inside the boundary layers and then we increase successively far in the bath. (Figure 1(b)). The three-dimensional calculations were performed at a steady state, with a constant liquid density assuming a laminar flow with the following thermo-physical parameters; H_2O at ambient conditions, with a diffusion coefficient $D=10^{-9}$ m^2/s.

To measure the performance of this electrode, we assume that the reaction rate at the surface is infinite, we apply a zero concentration on the electrode C = 0 at z = 0, for all the other surfaces we apply a bulk concentration of 1 (C = 1). A perfect sliding condition is applied to the upper free surface of the bath which is assumed to be plane.

The applicable range of angular speeds, ω, for the rotating disk electrode are {10, 50, 100, 150, 300,500} rd/s which correspond to Reynolds numbers, $Re=\omega r^2/\upsilon$, {70; 350; 600, 1051, 2170, 3510}. There is no real agreement about a critical laminar turbulent transition value of the Reynolds number in literature. Some mentioned critical Reynolds number, $Rec= 3.10^5$ [12], or $Rec=1.8\ 10^5$ [7]. Even if most authors of experimental studies agreed that turbulence appears earlier than the critical Reynolds values given in literatures [7,12,13], no work achieved a reliable methodology to identify the turbulence transition. As a first approach, we will consider that the flow is laminar.

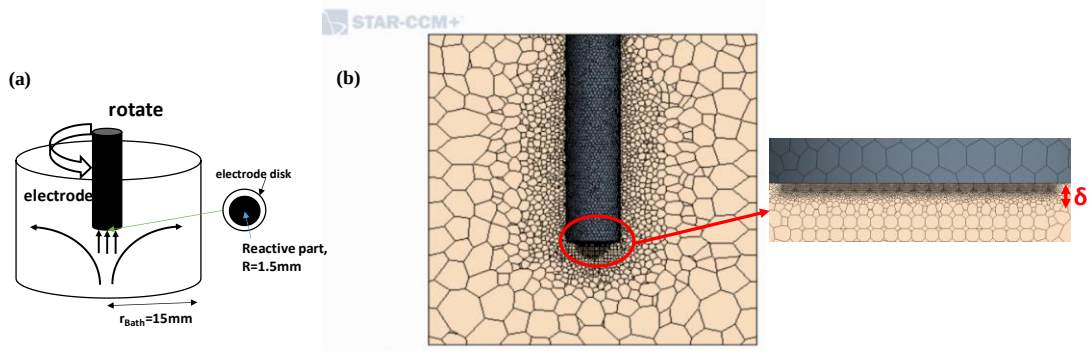

Figure 1: (a) schematic presentation of the electrochemical cell of r bath=1.5 cm, R electrode=1.5 mm, (b) Mesh representation of 2D cut for a 3D mesh (polyhedral) used in our calculation, with a detailed view near the electrode bottom.

4. RDE Numerical and Experimental Results

To investigate the efficiency of the mass transport of fluid in this actual cell, we study the influence of electrode rotation on the diffusion boundary layer, δ. For the electrochemical setup used in our laboratory, we run the simulation at a range of angular velocities from ω= 10 rd/s to ω=500 rd/s. To

validate our numerical results with experimental setup we choose a well-known, simpler and less expensive reaction than dehydrogenase enzymes: the oxidation of ferrocyanide in a bath containing a solution of (0.1 M) of $Fe(CN)_6^{4-}$ within a supporting electrolyte of sodium chloride (0.1 M). Once again, we reproduce the experimental setup (Figure 1). The electrode is performed by polishing the bottom surface (graphite type) with alumina and align the electrode vertically on the bath. Based on the relation between the current and the diffusion boundary layer, δ [3], we calculate δ from experimental results with our voltammetric measurements [14] at different rotational velocities as shown in Figure 2. We obtain a good agreement between the numerical, analytical and experimental results. With a RDE, the diffusion boundary layer is inversely proportional to the square root of the velocity. This may be an advantage in controlling this boundary layer, which is probably partly responsible for the success of this technology. But it is also, in our case, a limit as it becomes impossible to obtain a significant reduction of the boundary layer beyond 300 rd / s. Moreover, at high angular velocities> 300 rd / s, formation of instabilities in the solution is observed rather than an effective reduction of the diffusion boundary layer.

We have shown that RDE will not allow the detection of dehydrogenase enzymes action, as it would be unreasonable and inefficient to exceed speeds above 300 rd/s (about 3000 rpm) to achieve sufficient reagent transfer to the electrode. Nevertheless, this study demonstrates the validity of our numerical approach to simulate the hydrodynamics and the diffusion of species in the electrochemical cells.

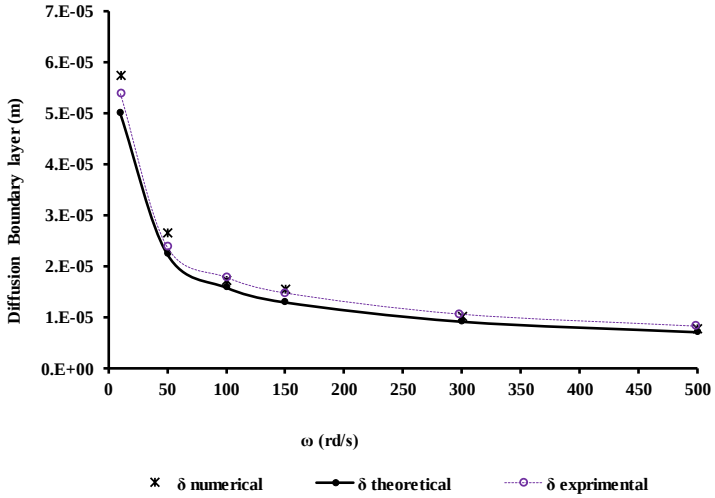

Figure 2: Enhancement of mass transport presented by the variation of the diffusion boundary layer, δ(m) versus the rotational velocities, ω(rd/s) ∈ (10 rd/s to 500 rd/s) numerical simulation, voltammetric experiments and analytical solution of Levich theory (equation 4).

5. Flow Cell Geometries:

Facing the limitation to use RDE, and in order to carry out an electrochemical study of the dehydrogenase it appears necessary to design a new cell ensuring a much better supply of reagents to the electrode. Other types of electrochemical cells described in the literature are based on the concept of a fixed electrode and a flow that ensures the supply of species. This supply can be parallel to the electrode in the case of "channel" type cells [15] or perpendicular to the cells of jet type [10]. Our goal is to obtain the highest and most homogeneous reagent flux by minimizing the diffusion boundary layer which must be regular along the surface of the electrode. It is also necessary to minimize the effects of washing the flow on the enzymes, but this part of our work will not be presented here.

5.1 Channel Flow Cell :

The conditions chosen for these simulations are similar to those used for the RDE, the concentration on the electrode is assumed to be zero, the concentration of the fluid at the inlet of the cell is equal to 1. This study is performed at low velocity, average velocity: v=0.02 m/s (laminar flow regime), which will be the same velocity used to represent the data of other configurations. The channel flow cell presented in Figure 3, is a half symmetric part to preserve energy and time in computation.

Figure 3 shows the numerical study for a classical channel electrode [15,16]. The geometrical configuration of the channel electrode is presented in Figure 3 (A). The obvious result from this simulation on the channel electrode, is the great heterogeneity of flux over the electrode surface as shown in the map of flux in Figure 3 (B). Where the flux is the transport limited current (A) divided by nFA, where n is the number of electrons transferred per redox event, F is the faraday constant (96485 C mol^{-1}), and A is the surface area of the electrode (m^2). The average flux at the electrode surface equals to 4.55 10^{-2} $kg.m^{-2}.s^{-1}$. For clear presentation of the flux, Figure 3 (C) represents the evolution of the mass flux along the line (D) at the electrode surface from the center to its edge, ranges from 0.027 to 0.1. The non-uniformity of the flux reaches more than 100%. Such a variation of flux on the electrode will generate unacceptable uncertainties of our experimental results.

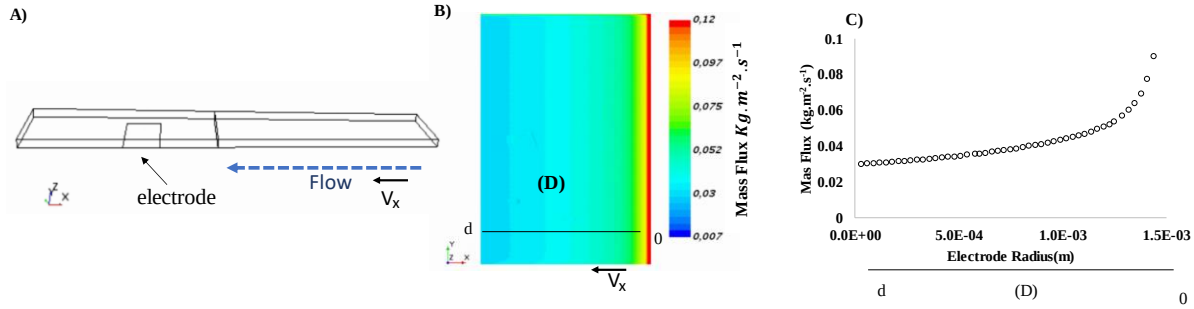

Figure 3: Numerical simulation study of Channel electrode: (A) geometric presentation of classical channel electrode cell, (B) flux distribution along the electrode surface (up view) and (C) flux at the electrode surface. Velocity of the flow is 0.02 m/s, radius of electrode = 3 mm.

5.2 Jet-Flow Electrode Cell

The channel electrode is considered as an efficient electrode but it is not adapted to our electrochemical analysis problem due to the non-homogeneity of the flux. Therefore, we study another type of electrode described in the literature as particularly efficient, the jet type electrode.

To optimize the flow in jet electrode cell, several factors must be taken into consideration in particular two main parameters: the distance between the end part of the inlet and the electrode surface, H, and also the geometrical configurations of the position of the outlet with that of the inlet and the shape of electrode.

5.2.1 The impact of the distance between inlet and the electrode surface:

Literature distinguishes two flow behaviors depending on the distance between the inlet and the electrode [17]: First case where the inlet is sufficiently far from the electrode surface so the fluid flow is not restricted and creates different regimes. With the raise of the velocity of the fluid exiting the inlet the probabilities of formation of vortices increase. A second case where the inlet is close to the surface, the flow is radial over the electrode surface preventing the formation of vortices and recirculation.

We simulate the 2D geometry as presented in Figure 4 (A). It is an axisymmetric cylindrical geometry of jet flow electrode type of diameter of inlet, a, equals to 3mm and radius of electrode=1.5mm.

Convection within the entire simulation domain is solved with Star CCM+ using the incompressible Navier-Stockes and continuity equations like in the previous geometries.

In this case, we address the impact of H, and we plot the variation of the diffusion boundary layer computed from our numerical simulation over a range of H values (from 5mm to 24 mm). This allows us to have the ratio of H/a at several volume flow rates.

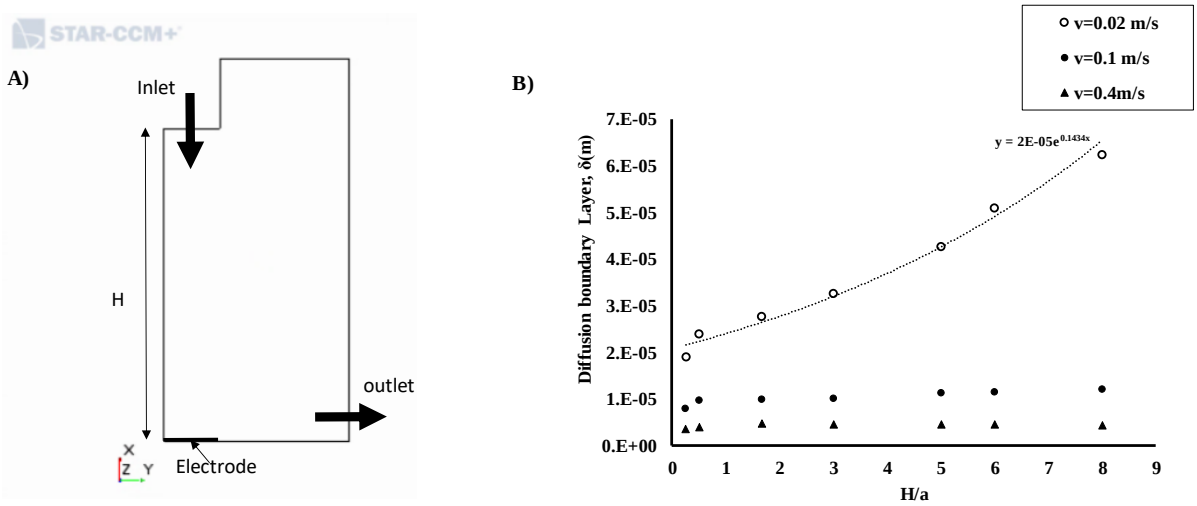

Figure 4 : (A) 2D axisymmetric Jet electrode (half part) of r inlet= r electrode= 1.5 mm, (B) A plot represents the variation of the calculated diffusion boundary layer from numerical simulation computed at velocities: v=0.02, 0.1, and 0.4 m/s with respect to the ratio of H/a.

Figure 4(B) shows the decrease of the diffusion boundary layer with the reducing of the distance between the inlet and the electrode surface at low velocity, v=0.02 m/s. While at higher velocities, the curve is almost constant independent of the ratio of H/a. We can conclude from this study that the small distance between the inlet and electrode surface is useful for lowering the diffusion boundary layer to get a better enhancement of flow and this impact is evident at low velocities. This is important in our case that impress us to be at very high flow rates to avoid the washing effect of the enzyme. Using the Microsoft tools, we express the variation of the diffusion boundary layer versus the ratio of H/a at low velocities, as this approximate relation: $\delta=2.\ 10^{-5}\ e^{0.143(H/a)}$. For the case of ratio H/a=0.5, we will work on this configuration to avoid the instabilities due to the very short distance at these strict boundary conditions.

5.2.2 Hydrodynamics of Practical Flow Cell with One Outlet

For a defined geometrical cell, we tested a practical design of small chamber bath, compatible with our study that resulted in a conclusion of the importance of having a small ratio of H/a, for better enhancement of flow toward the electrode surface. This design was based upon a currently available commercial package (DropSens, Spain). The system is composed of a central inlet nozzle and a single outlet nozzle aligned within an angle from the inlet.

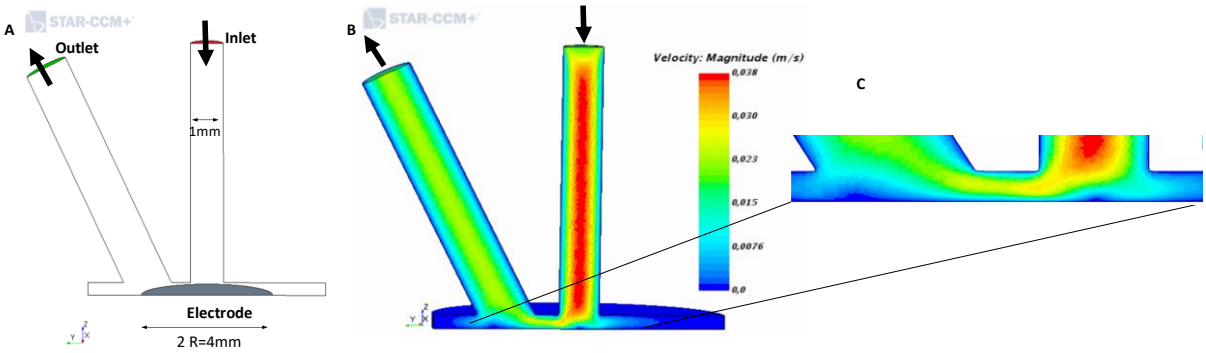

Figure 5: (A)Geometric scheme of the inlet centered above the electrode (R=2mm), H/a=0.5 and an outlet at an angle with the inlet, (B) hydrodynamic profile for the situation where the inlet confines the hydrodynamic flow rate, V_f=1 ml/min, v=0.02 m/s (C) the velocity profile within the domain close to the electrode.

The numerical simulations are performed with the same physical conditions of the previous computation (4.2). In Figure 5, the solution of velocity is well established in the inlet tube but quickly becomes distorted upon exiting the inlet, generating a higher solution speed at the leading inlet toward the outlet side. This impact is clearly observed further from the center of the inlet, with a stagnation effect at the furthest point from the outlet, although away from the electrode part.
Our interest is in the diffusion process near the electrode surface where the site of reaction and electron transfer process occurs. For that, our numerical study extends to study the concentration solution profile as shown in Figure 6(A). It represents the concentration profile in the whole system and within the domain near the electrode surface Figure 6 (B), which includes the diffusion boundary layer where the gradient of concentration starts to perform. For clear and qualitative analysis (Figure 6 (C), the concentration profiles are plotted along the axial distance toward the electrode surface (z-axis), where the gradient concentration ($\partial C/\partial z$) represents the slope of the curve. This slope is inversely proportional to the diffusion boundary layer thickness. As realized from Figure 6, the slope of the curves is highest at the center of electrode. Whereas, the slopes start to vary and decrease as getting away from the center of electrode, where it is not exposed to the inlet flow directly, furthermore, this is clearly observed and influenced in the area next to the outlet where the concentration profile is in a linear form. Thus, the diffusion layer is much bigger in this area by more than 10 times at the center of electrode. This can be enhanced by plotting the flux map at the electrode surface (Figure 6-D and E), The flux is concentrated in the area directly imposed to the inlet flow, thus the smallest diffusion boundary layer, then the flux starts to distribute along the electrode surface in asymmetric way, with the minimum value reached at the area next to the outlet. This can raise the issue of the impact of heterogeneity at the electrode surface, and the confidence of the measurement results from the experiments using this system. As a conclusion, based on the numerical simulation study, this geometrical configuration proves the asymmetric distribution of the flow and by that the flux at the electrode surface, in specific area of electrode not exposed directly to the flow.

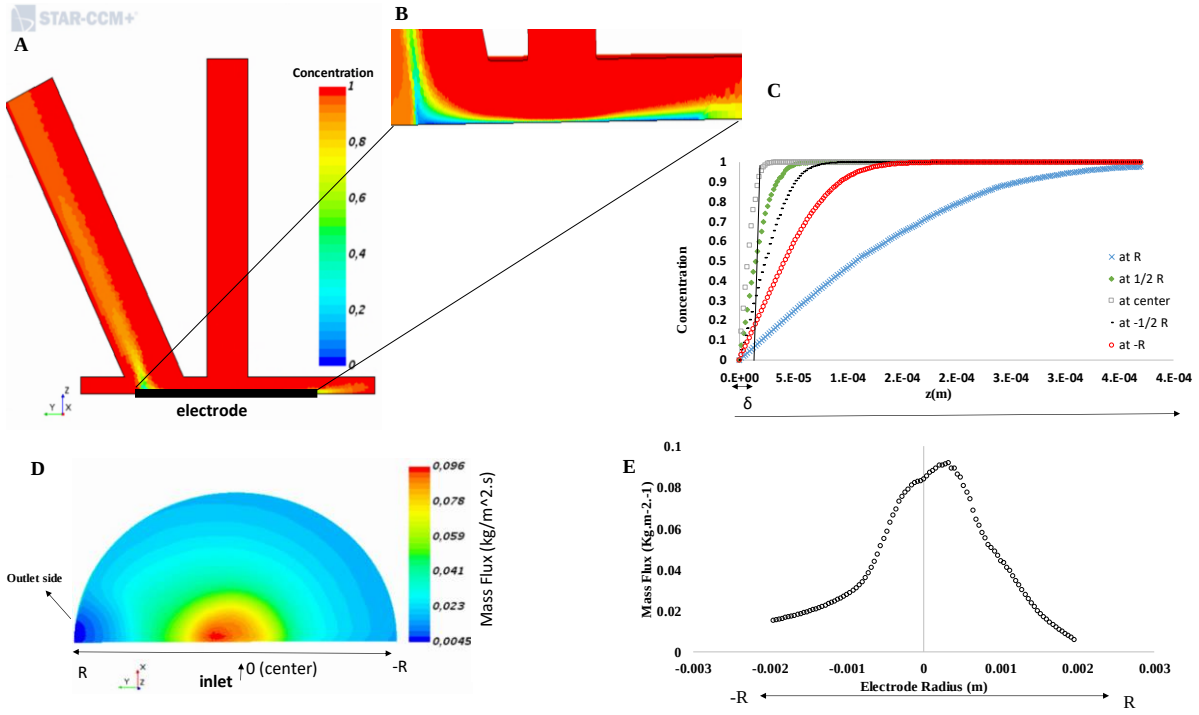

Figure 6: (A) the concentration profile predicted by simulation of convection and diffusion within the entire geometry and (b) the concentration profile calculated only within the domain close to the electrode, (C) represents the axial concentration profiles along the electrode surface (R=2 mm), with the representation of the diffusion boundary thickness layer (δ), (D) shows flux distribution at the electrode surface (top view of half symmetric part), and (E) a plot of the flux at the half part of the electrode surface. This numerical simulation is performed at v=0.02 m/s.

6. Two Nozzle Design

Previous studies were performed on a simple configuration where the inlet and outlet are in vertical alignment. They derive a conclusion on the numerical study of the velocity behavior of the fluid inside the cell, that the hydrodynamics established in this design are inadequate from true radial flow systems. Following that, they used to design their own cell consist of a central inlet and four symmetric outlets in vertical alignment with the inlet, that can fit their way of interest [17].

Regarding the results in the literature and our study that we performed on the practical commercial cell (previous section), guide us for a new design of flow cell. The successive optimizations we have carried out lead to a simple design able to be build and adequate for a practical use with the enzymes and electrode material used for our electrochemical studies. This configuration globally consists of an inlet diameter equals to that of the electrode diameter, with two symmetrical outputs at a certain angle and a distance from the inlet (Figure 7(A)).

To investigate the enhancement of the flow toward the reactive part at the electrode and address the heterogeneity, a representation of the flux distribution on the surface of the electrode is shown in Figure 7 (B), and a plot of the flux of line (D) at the surface of the electrode.

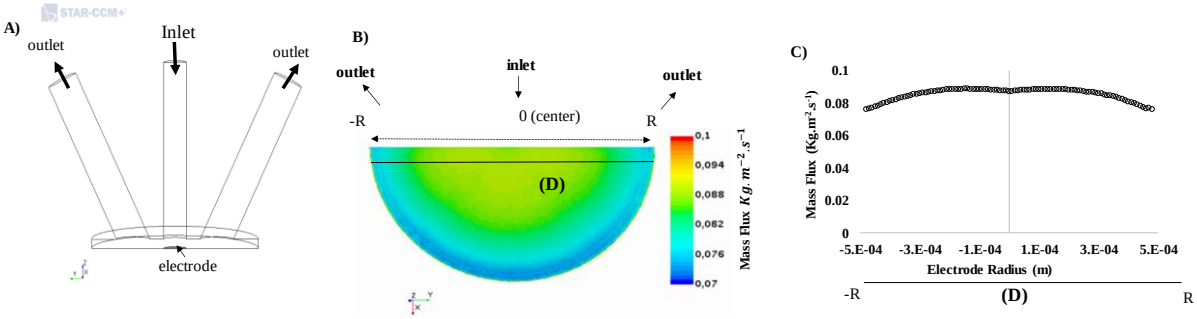

Figure 7: (A) Geometric presentation of symmetric outlet flow design with electrode radius, R =0.5 mm (cross section view), (B) mass flux map along the electrode surface (half symmetric part, top view), and (C) is a graph represents flux at the electrode surface, along the line (D). This numerical simulation is performed at v=0.02 m/s.

Herein, we represent shortly the important results of this configurations. Figure 7 summarizes the advantages of this new configurations over the presented geometries. Firstly, the homogeneity of the flux at the electrode surface is almost achieved. The flux variation at the surface of the electrode is less than 12%. This small variation is also visible in Figure 7 (C). This ensures the capacity of this configuration to avoid the distortion of the flow and solve the problems faced in the previous configurations (the detailed study and the impact of various parameters will be addressed later). Note also that the average flux obtained, equals to 0.082 $kg.m^{-2}s^{-1}$, represents the highest value on all the configurations that we tested, comparable to the channel flow cell, RDE and jet flow cells.

Among the different types of electrodes used in electrochemistry we have shown that the jet type electrode is best suited to our needs. Regarding our concerns, it exhibits a particularly high flux and homogeneity compatible with our experimental constraints.

7. Conclusion

We compared the main geometries of hydrodynamics electrodes types present in the literature. First, we show the limitations of RDE toward achieving enhanced transport of flow, verifying our methodology with analytical solution and our experimental results. Then, we present the incompatibility of channel flow cell due to a variation of flow on electrode. We investigate the capabilities of Jet flow electrodes and identify main parameters that must be optimized to control mass flow at the electrode, like jet diameter to electrode radius ratio and distance from jet inlet to the electrode surface. We tested a commercial jet flow cell that is efficient in term of global reaction rate but our simulations show that it will not behave enough homogeneous reaction on electrode to be applied to our enzyme study.
Then, we design a new jet electrode cell with two nozzle outlets, the simulation study shows very promising to our application. This prototype cell will be build and tested on our experimental apparatus, we will be able to study our enzyme but also to validate our simulation. The next step is better understanding the influence of main parameters of the cell to control the transport of reactive by modifying the velocity of the flow or the geometry of jet. We also need to study the wall shear stress on the electrode surface and its impact on enzyme washing that is actually unaddressed in literature.

References

[1] H. Dobbek, J.-H. Jeoung, Carbon Dioxide Activation at the Ni,Fe-Cluster of Anaerobic Carbon Monoxide Dehydrogenase, Science (80). 318 (2007) 1461–1465.

[2] C. Le, P. Bertrand, Direct Electrochemistry of Redox Enzymes as a Tool for Mechanistic Studies Direct Electrochemistry of Redox Enzymes as a Tool for Mechanistic Studies, Chem. Rev. 108 (2008) 2379–2438.

[3] R.G. Compton, C.E. Banks, Understanding Voltammetry, (2011).

[4] A.J. Bard, L.R. Faulkner, electrochemical methods fundemental and applications, second edi, 2001.
[5] M.E. Snowden, P.H. King, J.A. Covington, J. V. MacPherson, P.R. Unwin, Fabrication of versatile channel flow cells for quantitative electroanalysis using prototyping, Anal. Chem. 82 (2010) 3124–3131.
[6] K.; Stulik, V. Pacakova, Electroanalytical Measurements in Flowing Liquids, John Wiley and Sons,New York, NY, 1987.
[7] P. Mandin, T. Pauporté, P. Fanouillère, D. Lincot, Modelling and numerical simulation of hydrodynamical processes in a confined rotating electrode configuration, J. Electroanal. Chem. 565 (2004) 159–173.
[8] Q. Dong, S. Santhanagopalan, R.E. White, A Comparison of Numerical Solutions for the Fluid Motion Generated by a Rotating Disk Electrode, J. Electrochem. Soc. 155 (2008) 963.
[9] V. Levich, Physicochemical hydrodynamics., Prentice-Hall, Englewood Cliffs N.J., 1962.
[10] M.B. Glauert, The wall jet, J. Fluid Mech. 1 (1956) 625.
[11] W.J. Albery, S. Bruckenstein, Uniformly accessible electrodes, J. Electroanal. Chem. Interfacial Electrochem. 144 (1983) 105–112.
[12] C.I. Banks, A.O. Simm, R. Bowler, K. Dawes, R.G. Compton, Hydrodynamic electrochemistry: Design for a high-speed rotating disk electrode, Anal. Chem. 77 (2005) 1928–1930.
[13] J. Gonzalez, C. Real, L. Hoyos, R. Miranda, F. Cervantes, Characterization of the hydrodynamics inside a practical cell with a rotating disk electrode, J. Electroanal. Chem. 651 (2011) 150–159.
[14] C. Léger, Direct electrochemistry of proteins and enzymes: an introduction (2013).
[15] J. a. Cooper, R.G. Compton, Channel Electrodes-A Review, Electroanalysis. 10 (1998) 141–155.
[16] R.G. Compton, M.B.G. Pilkington, G.M. Stearn, Mass Transport in Channel Electrodes, 84 (1988) 2155–2171.
[17] M.E. Snowden, Electroanalytical Applications of Carbon Electrodes using Novel Hydrodynamic Flow Devices by Department of Chemistry Table of Contents, Film. (2010).